Analysis and Measurement of the Stability of Dual-Resonator Oscillators

Hassan Ghaed, Greg Chen, David Blaauw, Dennis Sylvester
University of Michigan, Ann Arbor, MI 48109, USA

***Abstract-* This paper investigates the stability of oscillators with dual-resonating tanks. After deriving oscillator models, it is shown that contrary to prior belief, there can be only one stable oscillating state. Sufficient conditions for stable oscillating states are derived and silicon measurement results are used to prove their validity. A fully integrated transmitter for intraocular pressure sensing that leverages the dual-resonator tank is designed and fabricated based on the derived models. An unstable version of the transmitter is also demonstrated to prove the concept of instability in dual-resonator oscillators when required conditions are not met.**

I. Introduction

Dual band communication systems have attracted attention with the introduction of new technologies in higher frequency bands. For example, wireless LAN has used the 2.4GHz band in its earlier versions but switched to 5GHz to achieve higher bandwidth [1]. Dual band transceivers allow compliance with both the old and new communication protocols.

In order to realize a dual band transceiver, the oscillator must be able to synthesize both frequencies of interest. Conventional single-tank oscillators have limited tuning range that cannot cover two different bands with significant separation. In addition, increasing the tuning range worsens phase noise [2]. Using a dual-resonating tank as shown in Fig. 1 can enable dual-band operation without sacrificing system performance. Compared to having two separate single-band oscillators, the dual-resonator architecture is more compact area achieves faster switching time.

Switching from a single-resonance tank to a dual-resonance tank changes the system dynamics. The question that arises is whether the oscillator will oscillator at the first, second, or both of the frequencies. In [3], the authors derived nonlinear models for the oscillator and concluded that the system can only oscillate at one of the two frequencies, which are both stable. They suggested that it is possible to switch between these two states by shorting either tank, allowing oscillations to form in the other tank. They proposed that the system will maintain oscillations at the same frequency when the switch is released.

This paper shows through additional analysis as well as measurement results that certain conditions must be satisfied for this to occur. In other words, either of the frequencies can become unstable if the dual-resonating tank is not properly designed. Two 0.18um CMOS oscillators were fabricated to validate this concept. Measurement results show instability in one of the chips at a designed frequency and stable operation at the other frequency.

The remainder of the paper is organized as follows. Section II models an oscillator with a dual-resonating tank and derives the necessary conditions for stable oscillating states. Section III explains the fabricated chip design procedure and includes the measurement results. Finally, Section IV highlights the conclusions of the paper.

II. Model Derivation

Fig. 1a shows the schematic of an oscillator with a dual-resonator tank. The non-linear voltage-dependent current source models the negative impedance provided by the cross-coupled differential pair. Resistances R1 and R2 are parallel resistances corresponding to the tanks. Note that both these resistances are frequency dependent and have different values at the two oscillation frequencies.

In order to form oscillations at ω_1, the second tank is shorted. Then the switch just used to short the second tank is opened to avoid the excessive phase noise it adds to the tank.

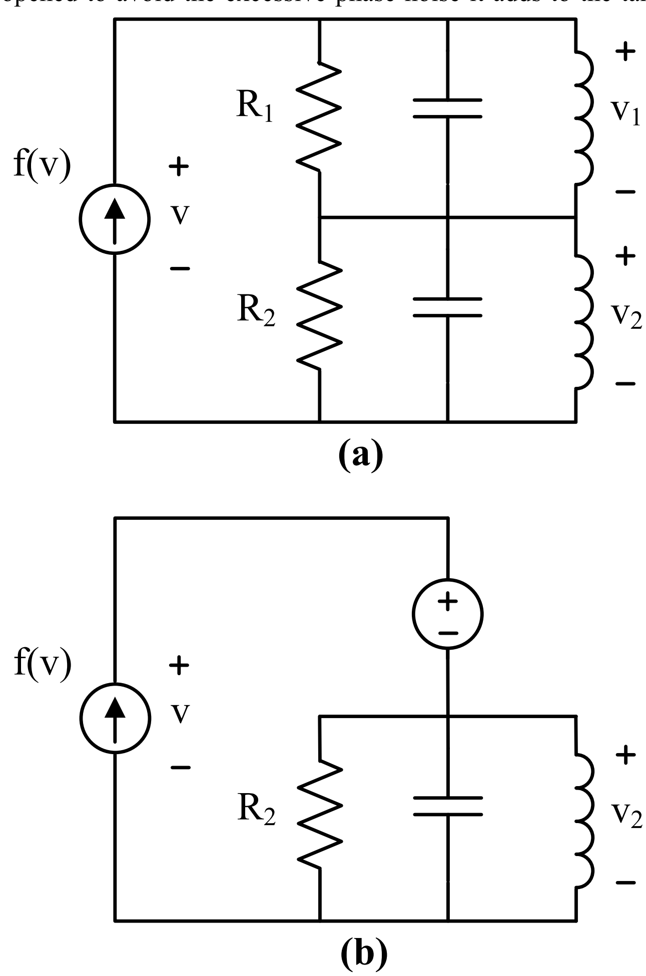

Fig. 1. (a) Schematic of an oscillator with a dual-resonator tank. (b) Simplified schematic to model the transient circuit behavior while the first tank oscillates with approximately constant amplitude.

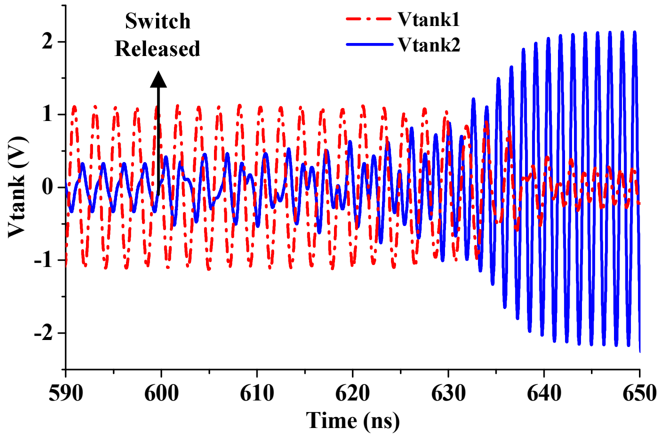

Fig. 2. Simulated voltages of a dual-resonator tank. After opening the switch that shorts the second tank, oscillations can develop at the second tank's frequency (ω_2), resulting in the loss of the previous state (ω_1).

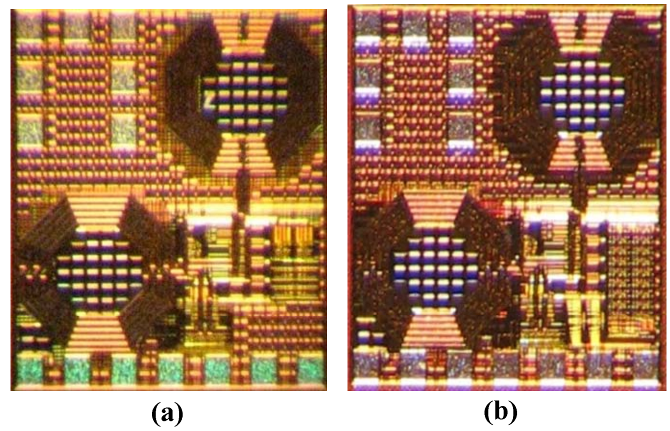

Fig. 3. Die photos of the unstable (a) and stable (b) dual-resonator transmitter designed in 0.18um CMOS for an intraocular pressure sensor transmitter.

The tank is expected to remain oscillating at ω_1. This is referred to as stable oscillation at that frequency. The authors of [3] comprehensively studied the state space of the system and derived the phase portrait for the system. However, the problem was oversimplified since the effect of tanks on each other during transitions was neglected. As shown in Fig. 2, oscillations at the first frequency can be unstable, in contrast to what was derived in [3]. Also note that the oscillation amplitude across the first tank is nearly constant until significant oscillations are formed in the second tank. Let us refer to the first tank as the aggressor and the second one as the victim. In other words, an unwanted instability occurs when the victim manages to form oscillations with the aggressor present. To simplify the problem, we can assume that until significant oscillations are formed in the victim tank, the aggressor acts as a sinusoidal source with constant amplitude A_1. The simplified schematic is shown Fig. 1b.

To analyze the simplified circuit, we begin by writing KCL equations at the victim tank node:

$$f(v) = i_R + i_C + i_L = \frac{v_2}{R_2} + C_2 \dot{v}_2 + \frac{1}{L_2}\int v_2 dt \tag{1}$$

Differentiation yields:

$$f'(v)\dot{v} = C_2 \ddot{v}_2 + \frac{\dot{v}_2}{R_2} + \frac{1}{L_2} v_2 \tag{2}$$

Modeling the negative impedance as

$$f(v) = k_1 v + k_3 v^3 \tag{3}$$

results in a form similar to the well-known van der Pol [4] equation:

$$(k_1 + 3k_3 v^2)\dot{v} = C_2 \ddot{v}_2 + \frac{\dot{v}_2}{R_2} + \frac{1}{L_2} v_2 \tag{4}$$

Note that k_1 is equal to the absolute value of the negative g_m presented to the tank while k_3 models the voltage-limited nature of the circuit. Applying KVL yields:

$$v = v_2 + A_1 Sin(\omega_1 t)) \tag{5}$$

Thus, we can re-write Eqn. (4) as:

$$(k_1 + 3k_3(A_1 Sin(\omega_1 t) + v_2)^2)(A_1\omega_1 Cos(\omega_1 t) + \dot{v}_2) = C_2\ddot{v}_2 + \frac{\dot{v}_2}{R_2} + \frac{1}{L_2} v_2 \tag{6}$$

To approximate the behavior of the victim tank oscillations in presence of the aggressor, we expand it and its derivative as suggested in [5]:

$$\begin{cases} v_2 = A_2 Sin(\omega_2 t)) \\ \dot{v}_2 = A_2 Cos(\omega_2 t)) \end{cases} \tag{7}$$

The differential equation can be expanded to the first order to the form:

$$C_2\ddot{v}_2 + \frac{1}{L_2} v_2 = (k_1 + \frac{3}{4}k_3 A_2^2 + \frac{3}{2}k_3 A_1^2 - \frac{1}{R_2}) A_2 \omega_2 Cos(\omega_2 t) \tag{8}$$

The condition to avoid self-excitation [5] is given by:

$$\bar{\lambda}_{(0)} = \frac{1}{R_2} - \frac{3}{2}k_3 A_1^2 - k_1 > 0 \tag{9}$$

Assuming transistor transconductances k_1 and k_3 are independent of frequency, we can further simplify the condition. We can derive the value of A_1 as the limit cycle amplitude in van der Pol equation [6] at the first frequency:

$$\frac{3}{2}k_3 A_1^2 = \frac{2}{R_{1(\omega_1)}} - \frac{2}{k_1} \tag{10}$$

Substituting Eqn. (9) into Eqn. (8) results in:

$$\frac{2}{R_{1(\omega_1)}} - \frac{1}{R_{2(\omega_2)}} > g_m \tag{11}$$

Hence, as long as the frequency separation is low enough that the frequencies do not have different g_m values, Eqn. (11) describes the necessary condition for stable oscillations at the first frequency, ω_1. Similarly, in order to have stable oscillations at ω_2 the following condition must hold:

$$\frac{2}{R_{2(\omega_2)}} - \frac{1}{R_{1(\omega_1)}} > g_m \tag{12}$$

III. Design and Measurement Results

To verify the validity of the derived model, two chips with identical inductors were designed and fabricated in the same 0.18um CMOS process. Chip micrographs of both chips are shown in Fig. 3. The goal of the design was a fully integrated inductive coupling transmitter using the coils as transmission coils in an inductive link. By integrating the oscillator and power amplifier (PA), the stringent area constraint imposed by the implantable sensor application was met. The designed transmitter was used as a part of an intraocular pressure sensor presented in [7]. The dual-resonator architecture enables implementation of FSK modulation with two highly separated frequencies, thus relaxing the constraints on phase noise and resulting in better BER.

As suggested by Eqn. (11), one way to avoid oscillations is to reduce the absolute value of the negative g_m presented to the tank. In other words, oscillators designed in the voltage-limited regime are more likely to become unstable due to their excessive g_m. Note that in the transmitter designed for the intraocular pressure sensor, we preferred higher absolute g_m values so that more power is delivered to the coil and higher transmission distances can be achieved. In this way, there is a trade-off between stability and the amount of power delivered to the coils.

Another approach to achieve stability at ω_1 is to decrease R_1 in Eqn. (11). However, decreasing R_1 is equivalent to reducing the quality factor of the tank. This results in lower transmission range and higher phase noise in the inductive link, which is not acceptable.

Fig. 4 shows measurement results for a dual-resonator

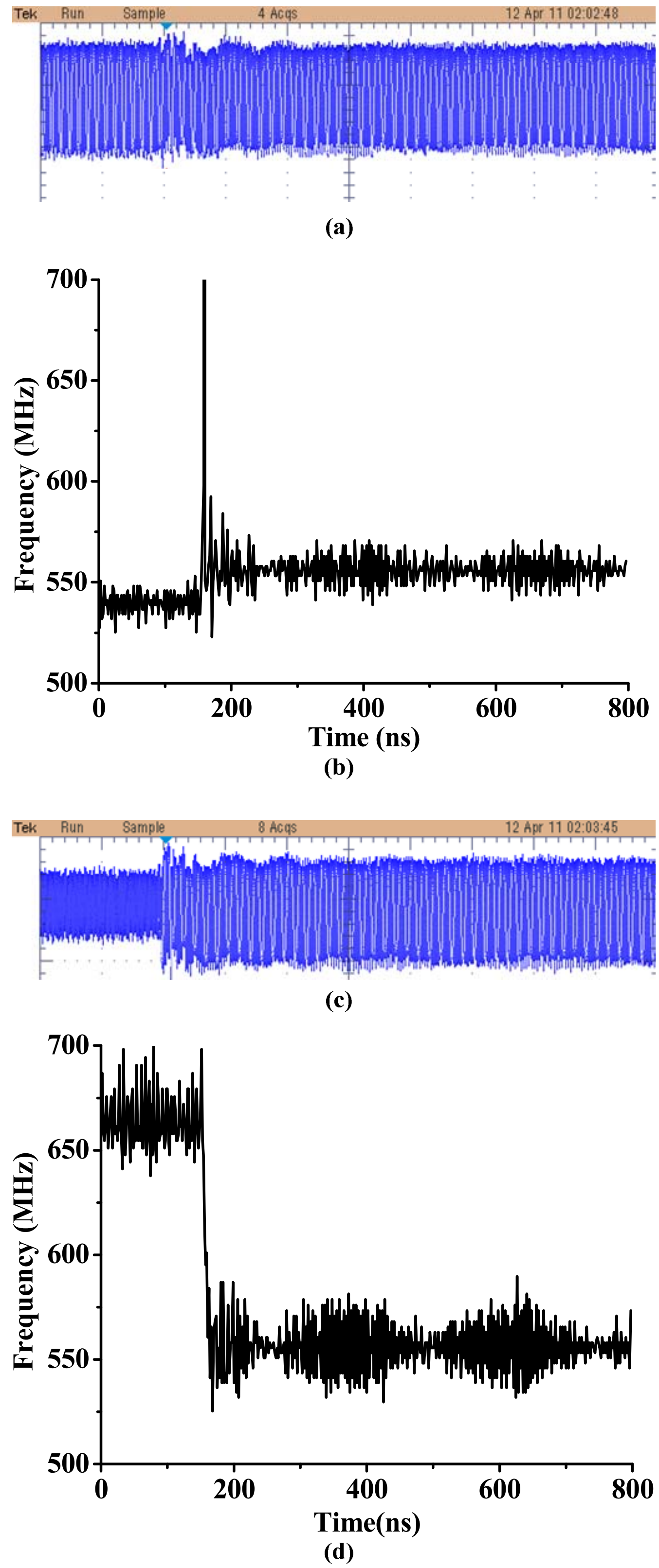

Fig. 4. Unstable oscillator results. Normalized dual-resonator tank voltage (a,c) and frequency (b,d) when the switch shorting the non-oscillating tank is opened. The first tank (a,b) keeps oscillating at the original frequency. The second tank (c,d) is unstable. Oscillations develop on the previously shorted tank and the dual-resonator starts to oscillate at the new frequency.

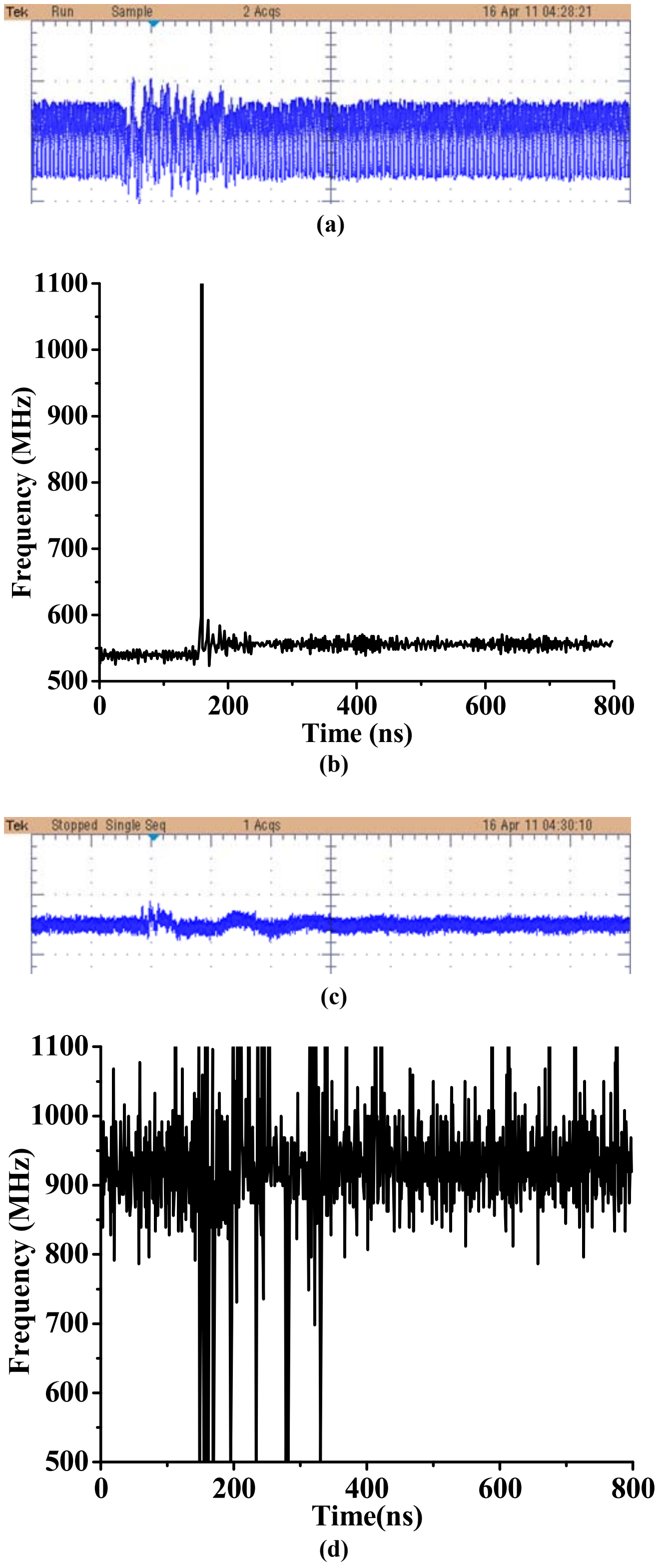

Fig. 5 . Stable oscillator results. Normalized dual-resonator tank voltage (a,c) and frequency (b,d) when the switch shorting the non-oscillating tank is opened. In both cases, the tank keeps oscillating at the original frequency.

oscillator with f_1=540 MHz and f_2=660 MHz that was intentionally designed to be unstable at f_2 (Fig. 3a). As shown in Fig. 4a and 4b, oscillations at f_1 are stable as the dual-resonator continues to oscillate at the same frequency upon releasing the switch shorting the second tank. This is not the case for oscillations at f_2, as seen in Fig. 4c and 4d. The oscillation frequency changes after the switch shorting the first tank is opened, because the g_m value is high enough to suppress the pre-existing state.

Fig. 5 shows measurement waveforms for the second version of the oscillator using identically designed inductors and different frequency separation. This time, the transmitter can hold its state after either of the switches shorting the tanks is opened, thereby achieving fully stable operation.

Let us examine the validity of the model by checking the stability conditions in our two chips at the higher frequencies. Since the frequencies are highly separated, we cannot use the simplified equations. Re-writing Eqn. (9) for the second frequency gives us the stability criteria for ω_2:

$$\frac{1}{R_1}-\frac{3}{2}k_3A_2^2-k_1=\begin{cases}-0.79\,mmho>0 & \text{first chip}\\ +0.74\,mmho<0 & \text{second chip}\end{cases}\qquad(13)$$

We have used simulation results to extract the required parameters at the two upper frequencies. Note that the stability condition is only satisfied for the second chip. This is in agreement with our measurements in Fig 4.d and Fig 5.d.

V. Conclusion

As was shown through silicon and simulation results, designing oscillators with dual-resonator tanks can be challenging due to the possibility of state loss that was previously unknown. This work derived a model that describes the conditions that must be satisfied to guarantee a robust design. We showed that the choice of the negative transconductance, tank quality factors, and frequency separation impact the ability of the system to holds its state.

Acknowledgments

The authors would like to thank Professor Khaled Salama for his insightful help. The authors would also like to gratefully acknowledge partial project funding from the King Abdullah University of Science and Technology.

References

[1] T. Ruhlicke, M. Zannoth, B.U. Klepser, "A highly integrated, dual-band, multi-mode wireless LAN transceiver," *IEEE European Solid-State Circuits Conference*, pp. 229- 232, Sept. 2003.

[2] L Romano, V. Minerva, S.C. d'Oro, C. Samori, M. Politi, "5-GHz in-phase coupled oscillators with 39% tuning range," *IEEE Custom Integrated Circuits Conference*, pp. 269- 272, Oct. 2004.

[3] A. Goel, H. Hashemi, "Frequency switching in dual-resonance oscillators," *IEEE Journal of Solid-State Circuits*, vol.42, no.3, pp.571-582, Mar. 2007.

[4] B. van der Pol, "The nonlinear theory of electric oscillations," *Proceedings of the IRE*, vol. 22, no. 9, pp. 1051–1086, Sept. 1934.

[5] N. Kryloff and N. Bogoliuboff, *Introduction to Nonlinear Mechanics*. Princeton, NJ: Princeton Univ. Press, 1947.

[6] D. B. Leeson, "A simple model of feedback oscillator noise spectrum," *Proceedings of the IEEE*, pp. 329–330, Feb. 1966.

[7] G. Chen, H. Ghaed, R.M. Haque, M. Wieckowski, Y. Kim, G. Kim, D. Fick, D. Kim, M. Seok, K. Wise, D. Blaauw, D. Sylvester, "A cubic-millimeter energy-autonomous wireless intraocular pressure monitor," *IEEE International Solid-State Circuits Conference*, pp.310-311, Feb. 2011.